Rossby Wave Generation by Poleward Propagating Kelvin Waves: The Midlatitude Quasigeostrophic Approximation

JOHN D. McCALPIN

The Graduate College of Marine Studies, University of Delaware, Newark, Delaware

(Manuscript received 13 October 1993, in final form 14 October 1994)

ABSTRACT

The phenomenon of Rossby wave generation by poleward propagating baroclinic coastal Kelvin waves is discussed in the low-frequency quasigeostrophic (QG) limit. The response of the system is divided into three frequency regimes: a low-frequency regime (longer than annual periods) for which the previously studied long-wave models are quite accurate, a high-frequency regime (semiannual or shorter) for which the Kelvin waves are coastally trapped (and thus of negligible importance to the interior), and an intermediate regime for which dispersive effects are important to the scattering process.

It is shown that the retention of the y dependence of the radius of deformation in a locally 1D, QG model is necessary and sufficient to describe the dominant energy flux out of the coastal waveguide for all three of these frequency regimes. This Rossby wave energy flux directly determines the interior Rossby wave amplitudes and modifies the evolution of the Kelvin wave amplitude along the coast.

The result of the application of a QG midlatitude β-plane model to this scattering process is contrasted with more accurate results from the locally 1D QG model and from a generalized QG model (which retains the linear variation of Coriolis force with latitude in all terms). A direct numerical simulation of the reduced-gravity shallow-water equations is used as a reference. It is shown that the traditional assumption of constant deformation radius in QG models causes O(1) errors in the Rossby wave response in the interior, and somewhat smaller errors in the prediction of the changes in the coastal Kelvin wave amplitude.

1. Introduction

Coastal Kelvin waves are exact solutions of the linear, constant-coefficient (i.e., f plane) shallow-water equations. They are an unusual dynamical hybrid, obeying geostrophic dynamics in the cross-shore momentum balance and simultaneously obeying gravity wave dynamics in the alongshore momentum balance. In the presence of slowly varying environmental parameters, the Kelvin wave is reduced to an approximate solution, and its interaction with the other modes of the system is of intrinsic dynamical interest. The physical situation addressed here is the "leakage" of energy from low-frequency, poleward propagating coastal Kelvin waves into the interior Rossby wave field caused by the meridional increase in the Coriolis parameter. This has been the subject of several previous studies, particularly in regard to the oceanic behavior off the west coast of North America.

In this work, I present a simple model describing this interaction in terms of local midlatitude quasigeostrophic (QG) dynamics and discuss the potential and limitations of traditional limited-area, midlatitude QG models in representing this scattering process.

Section 2 reviews prior work on this topic. Section 3 reconsiders the long-wave model used by previous investigators. Section 4 adds dispersive corrections to the long-wave model results. Section 5 presents the results of the time-dependent, fully dispersive one-dimensional QG model. Section 6 investigates the y dependence of the solution using energy flux conservation arguments. The paper concludes with a discussion of the implications of these results for midlatitude QG modeling.

2. Prior studies

A large number of studies have attempted to understand the interior baroclinic variability of the subtropical and midlatitude northeast Pacific Ocean in terms of long, linear Rossby waves. Early studies (e.g., Roden 1977; White 1977; Meyers 1979; White and Saur 1981) generally interpreted the generation mechanism to be direct wind forcing. The demonstration by Enfield and Allen (1980) that sea level variability along the west coast of Central and North America is dominated by coherent, low-frequency Kelvin waves led to the later consideration of coastal sea level changes as a Rossby wave forcing mechanism. White and Saur (1983) investigated the roles of local and coastal forcing

Corresponding author address: Dr. John D. McCalpin, College of Marine Studies, University of Delaware, Robinson Hall, Newark, DE 19716-3501.
E-mail: mccalpin@perelandra.cms.udel.edu

in their analysis of XBT data from the San Francisco to Hawaii great circle transect. Considering interannual variability, they found forcing from the coastal sea level to be important south of 30°N, while this signal was not apparent north of 30°N. In more recent work, Shriver et al. (1991) make use of a complex EOF analysis to investigate the Rossby wave response to coastal Kelvin waves in the northeast Pacific, focusing on the 300-m temperature anomalies along 40°N, between 125° and 135°W. Rossby waves generated by the coastal Kelvin waves are inferred to contribute 47.5% of the variance of the 300-m temperature anomalies.

A number of analytical studies also relate to this problem, although they are generally posed for the wind-forced, rather than the boundary-forced problem. Anderson and Gill (1975) explore the adjustment of a stratified midlatitude ocean to an impulsively applied wind stress under both the f-plane and β-plane approximations. They note that the Kelvin waves generated by this wind are damped on the β plane due to energy leakage into the Rossby wave field and provide an analytic solution to the linear problem for a north–south wind on a β plane. Several studies using the equatorial β-plane approximation are also relevant, including the solution of Moore (1968) for equatorial Kelvin wave reflection from a meridional boundary. Moore shows that for sufficiently large y, the solution asymptotes to a coastal Kelvin wave trapped to within one internal deformation radius of the coast (i.e., there is no Rossby wave emission from the coastal waveguide poleward of a frequency-dependent "critical latitude"). This work is extended to the case of a step-function equatorial Kelvin wave by Anderson and Rowlands (1976). From the exact solution they observe a growth in the Kelvin wave amplitude proportional to $y^{1/2}$ due to conservation of energy. McCreary (1976) discussed the generation of Rossby waves by the leakage of ENSO-generated coastal signals in the context of the equatorial β-plane model. A comprehensive work by Grimshaw and Allen (1988) derives an equation for the low-frequency pressure evolution along variable geometry boundaries in a frequency-domain version of the linear, reduced-gravity equatorial β-plane equations. They use this theory to discuss the role of coastline geometry on the trapping of the coastal Kelvin waves. Other recent work provides somewhat simpler analyses for the case of nonmeridional boundaries (Clarke and Shi 1991; Clarke 1992) based on boundary-layer theory. These latter three references all point out that nonmeridional boundaries can shift the critical latitude away from that predicted by QG theory.

Modeling studies include the baroclinic long-wave model of White and Saur (1983), with latitude-dependent phase speed (both the stratification and Coriolis parameter varied in y). This model extended an earlier wind-forced model (White 1977) to include forcing by variations in sea level along the Pacific coast of Central America. The White and Saur model gave reasonable agreement with the low-frequency component of their interior oceanic observations. The later paper notes that the long-wave model is QG and that the sea level must be constant along the boundary for this quasigeostrophic model to be valid. The data show that this is approximately true. This issue will be addressed in section 5.

Pares-Sierra and O'Brien (1989) simulated the California Current region using a reduced-gravity primitive equation model with realistic geometry and wind forcing. A novel aspect of this simulation was the introduction of energy from an equatorial model along the coastal waveguide at the southern edge of the domain. They note that in the locally forced model, the annual period motions appear to be coastally trapped north of about 35°N. This is attributed to the sloping coastline modifying the theoretical value of approximately 40°N. There is also some evidence of trapping in the remotely forced model, but this is not separately discussed. Unfortunately, the model's geometric complexity and the presence of nonnegligible levels of viscosity make it difficult to quantitatively assess the mechanism(s) involved. This model was applied to the same region in a study of the influence of the 1982–1983 El Niño by Johnson and O'Brien (1990).

Several simulations of the region have employed QG models—in each case neglecting the mechanism of eastern boundary forcing via coastal Kelvin waves. Cummins and Mysak (1988) studied the northeast Pacific in the region north of 45°N, using a three-layer quasigeostrophic model. The southern boundary of their model is north of the critical latitude for annual waves, but not for the 3–4-year periods characteristic of ENSO-induced sea level variability, which have a critical latitude near 55°N (Clarke and Shi 1991). Another recent model is the nested northeast Pacific model of Holland and Vallis (1991, unpublished manuscript), covering the domain from 10° to 60°N, 90°W to 120°E. This QG model uses eight layers and is configured in spherical coordinates. Auad et al. (1991) perform an energy budget analysis of this model applied to a study of the California Current region, but the application of this analysis to the area is problematical due to the exclusion of forcing via coastal Kelvin waves.

3. The low-frequency model

The derivation in this section is simple, but it differs in a number of important ways from the prior literature in order to more directly address the relationship of the Kelvin wave scattering process to midlatitude QG dynamics. In particular, I emphasize the difference between the long-wave approximation and the low-frequency approximation, recognizing that an important component of the low-frequency solution (i.e., the coastal Kelvin wave) exists at short spatial scales. Therefore some care must be taken in deciding exactly where to make the long-wave approximation. The di-

rect numerical simulations of the shallow-water equations (SWE) will clarify the limits of applicability of these scalings. The discussion here is much simpler than the very thorough and rigorous analysis of Grimshaw and Allen (1988) (based on ray theory), but has the advantage of providing clear physical insight while containing errors no greater than those already incurred by the assumptions of linearity, uniform geometry, flat bottom, and spatially uniform stratification. The current discussion also differs from the theory of Moore (1968) (based on a meridional mode expansion of the solutions to the equatorial β-plane equations) by considering only local midlatitude dynamics.

We consider a uniformly stratified β-plane ocean with a closed boundary on the east. The domain is "open" to the north and south, and may be considered to be either open or of infinite extent to the west. A poleward propagating coastal Kelvin wave is imposed along the southern boundary ("leaning" against the eastern closed boundary) in exact geostrophic balance at that latitude. For Kelvin wave periods much longer than one pendulum day, imbalances created by variations of the Coriolis force along the path of the Kelvin wave propagation will result in the generation of Rossby waves, plus perhaps some coastally trapped (evanescent) waves. Only the Rossby waves will result in energy propagation into the interior, and those can be treated with a nearly geostrophic model.

For small amplitude solutions, the baroclinic behavior is governed by a set of "equivalent barotropic" (also called "reduced gravity") shallow-water equations. I choose the set corresponding to first baroclinic mode phenomenon off the west coast of North America, with an internal gravity wave phase speed of $\sqrt{g'H} = 2.4$ m s^{-1} (about 200 km per day). The linear β-plane equations are thus

$$u_t - (f_0 + \beta y)v + g'h_x = 0 \tag{1}$$

$$v_t + (f_0 + \beta y)u + g'h_y = 0 \tag{2}$$

$$h_t + Hu_x + Hv_y = 0. \tag{3}$$

The usual notation is used, with $g' = g\Delta\rho/\rho_0$ being the reduced gravity, H being the reference thickness of the upper layer of the ocean, and h being the vertical displacement of the layer interface, or oceanic thermocline.

To obtain the nearly geostrophic model, the exact f-plane Kelvin wave solution is subtracted from this β-plane system. The second and third equations remain unchanged (since the Kelvin wave solution remains an exact balance there even on the β plane), but it no longer produces an exact balance in the first equation. The imbalance results in a forcing term in the u-momentum equation for the "non-Kelvin" part of the solution:

$$u_t - (f_0 + \beta y)v + g'h_x = \beta y V_K. \tag{4}$$

This forcing term is the β term from the imbalance of the Kelvin wave as it propagates away from its initially balanced latitude. Assuming near geostrophy in the remainder of the solution, a generalized QG equation may be derived following the method of Williams (1985):

$$\nabla^2\eta_t - \frac{(f_0 + \beta y)^2}{gH}\eta_t - \frac{2\beta}{(f_0 + \beta y)}\eta_{yt} + \beta\eta_x = -\beta\phi_x + O\left(\frac{\beta y}{f_0}\right), \tag{5}$$

where ϕ is the thermocline anomaly of the f-plane Kelvin wave solution. For clarity, the symbol h will be used for the interface anomaly of the SWE model, while the symbol η will be used for the corresponding variable of the QG model. There are three additional terms of $O(\beta y/f)$ in the rhs of the vorticity equation that will be neglected hereafter. Although it does not appear to be formally consistent to neglect these terms while retaining the variations in the deformation radius on the lhs, the results presented later will show that neglect of the small forcing terms causes only small errors, whereas the neglect of variations in the deformation radius causes large errors.

For this nearly geostrophic model, we still need to determine the characteristic scales to see if further simplifications are possible. First, the y scale will be assumed to be much larger than R_d. Later, an energy flux analysis of the solution will demonstrate that the y scale is the smaller of the planetary scale, f_0/β, and the f-plane Kelvin wave scale, $\sqrt{g'H}/\omega$, which is very large at low frequencies (about 12 000 km at annual periods for $\sqrt{g'H} = 2.4$ m s^{-1}).

Second, we will assume that the length scale in the offshore (x) direction is the scale of the long free Rossby waves at the same frequency as the forcing:

$$k = \frac{1}{2\omega}\left[-\beta + \sqrt{\beta^2 - 4\omega^2\gamma^2}\right]. \tag{6}$$

Note that $\gamma \equiv f(y)/\sqrt{g'H} \equiv 1/R_d$ is the inverse of the deformation radius and that it is latitude dependent. For low frequencies, this asymptotes to the long-wave relation used by White and Saur (1983):

$$\frac{1}{k} = -\frac{\beta R_d^2}{\omega}, \tag{7}$$

which, in more familiar form, specifies a long-wave phase speed $c = -\beta R_d^2$, but which is a quadratic function of y through the f dependence of R_d.

Given these assumptions, the vorticity equation for the interior solution reduces to

$$\eta_t - \beta R_d^2\eta_x = \beta R_d^2\phi_x. \tag{8}$$

Note that this is not exactly the same as the long-wave equation of White and Saur (1983) in that the forcing is an *interior* forcing, rather than a *boundary condition.*

The correct boundary condition for this equation is $\eta(x = 0, t) = \delta(y, t)$, where δ is the difference between the actual amplitude of the Kelvin wave signal at a given latitude and the assumed amplitude on the rhs of (8). If the Kelvin wave signal were exactly constant along the coast, then the correct boundary condition would be $\eta(x = 0, t) = 0$, because the inhomogeneous part of the boundary condition (i.e., sea level variation) is associated with the Kelvin wave solution, which has already been subtracted off (at least approximately). The energy flux analysis presented later will show that $\delta \ll \eta$ for frequencies below the critical frequency and y locations within a few thousand kilometers of the location of the assumed f-plane Kelvin wave balance; therefore, $\eta(x = 0, t) = 0$ will be the boundary condition applied here. Note also that this equation is only parametrically dependent on y through the $R_d(y)$, and weakly through $\delta(y)$. Therefore, the dominant part of the y dependence of the solution must be determined independently, which will be accomplished in section 6 by consideration of the conservation of energy flux.

The long-wave vorticity equation, (8), may be solved by the method of characteristics. The forcing chosen is a unit-amplitude Kelvin wave

$$\phi(x, t) = \begin{cases} 0, & t < 0 \\ e^{\gamma x} \sin\omega t, & t \geq 0. \end{cases} \tag{9}$$

The solution is

$$\eta(x, t) = \frac{\gamma c}{\gamma^2 c^2 + \omega^2}\left[\gamma c \sin\left(\frac{\omega}{c}(x + ct)\right) + \omega \cos\left(\frac{\omega}{c}(x + ct)\right) - e^{\gamma x}(\gamma c \sin\omega t + \omega \cos\omega t)\right], \tag{10}$$

where $c \equiv -\beta R_d^2$. The solution is valid for the region $t \geq 0$ and $-ct \leq x \leq 0$, outside of which the solution is zero. Clearly, the first two terms are the propagating solution in the interior, while the last two terms are the directly forced solution in the coastal waveguide. The solution differs from that of the boundary-forced, long-wave model, which does not contain the cosine or directly forced terms.

In the interior, the maximum of the solution is

$$|\eta|_\infty = \left[1 + \left(\frac{\omega}{\gamma c}\right)^2\right]^{-1/2}, \tag{11}$$

which takes on the values

$$\omega \ll \gamma c \rightarrow |\eta|_\infty = 1 \tag{12}$$

$$\omega \gg \gamma c \rightarrow |\eta|_\infty = \frac{1}{\omega} \tag{13}$$

$$\omega \equiv \gamma c \rightarrow |\eta|_\infty = \frac{1}{\sqrt{2}} \tag{14}$$

for the specified values of ω. The transfer function implied by (11) is that of a first-order low-pass filter. Its magnitude is presented as the solid line in Fig. 1.

In the low-frequency limit, the free-wave part of the solution (10) is exactly the same as that for the boundary forcing employed by White and Saur (1983). However, as the frequency increases, this model predicts a decrease in the amplitude of the emitted Rossby waves, while the White and Saur (1983) model predicts a constant, unit amplitude. The decrease in amplitude with frequency is easily understood in the context of the characteristic method used for the solution. The solution is the integral along the characteristic path, $(x + ct) = \text{const}$, from the eastern boundary to the point of interest. At low frequencies, the forcing function is essentially constant during the interval $1/(\gamma c)$ required to traverse the R_d-scale coastal waveguide. As the frequency increases, the Kelvin wave varies in time along the characteristic, resulting in partial cancellation of the integrated effect of the forcing.

4. Dispersive corrections to the long-wave model

The low-frequency model just presented is formally limited to low frequencies by the long-wave approximation to the dispersion relation, so that its applicability at increasing frequencies is suspect. However, it is easy to see that the effect of dispersion is to *increase* the effect of the cancellation along the characteristics, and thereby *decrease* the Rossby wave amplitudes, by noting that dispersion acts to *slow down* shorter waves. This gives more time for the Kelvin wave forcing to vary while the information is being integrated across the coastal waveguide.

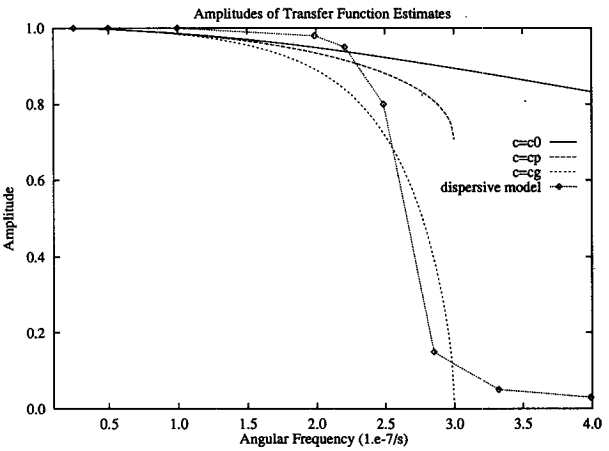

FIG. 1. Magnitude of the Rossby wave response to a unit amplitude Kelvin wave as a function of ω for several models: $c = c_0$ is for the long-wave model with the long-wave phase speed, $c = c_p$ is for the long-wave model using the frequency-dependent phase speed, and $c = c_g$ is for the long-wave model using the frequency-dependent group velocity. The curve labeled "dispersive model" gives the average value of the peaks in the range from -4000 to -1000 km after 16 years of integration of the fully dispersive model.

The low-frequency model can be extended to higher frequencies by considering single-frequency forcing (and solutions), rather than the more general case allowable by the method of characteristics. This approach was also used by Grimshaw and Allen (1988). For each forcing frequency, the phase speed can be replaced by the phase speed of the β-plane Rossby wave of the same period, using the wavenumber from (6) rather than (7). The amplitude of the transfer function is then

$$|\eta|_\infty = \left[1 + \frac{1}{4}\frac{(\beta + \sqrt{\beta^2 - 4\gamma^2\omega^2})^2}{\omega^2\gamma^2}\right]^{-1/2}, \quad (15)$$

which is plotted as the dashed line in Fig. 1. This function is seen to decrease somewhat more rapidly than the long-wave model transfer function. The function reaches a limiting value of $1/\sqrt{2}$ for $\omega = 3 \times 10^{-7}$ s^{-1}. For higher frequencies, no real solutions of (6) exist, indicating that no free Rossby waves exist for higher frequencies.

An alternative approach to modifying the long-wave model for higher frequencies is to use the group velocity for free waves at frequency ω, rather than the phase velocity as discussed above. This can be expected to give more reasonable results for the initial "turn on" of the model, for which energy propagation provides the appropriate dynamical control on the system. The results for this modification of the model are presented in the dotted curve of Fig. 1. This model suggests that the amplitude of the emitted Rossby waves will smoothly drop to zero at the critical frequency, at which point the Rossby waves have no westward group velocity, and therefore no ability to carry energy out of the coastal waveguide.

These results are in precise agreement with previous studies, such as Clarke and Shi (1991), who present the same critical frequency

$$\omega_c = \frac{\beta c}{2f}. \quad (16)$$

This is determined from the one-dimensional QG equation, [their (6)], just as here, and confirmed by analysis of the equatorial β-plane modes. Clarke and Shi note that the neglected y-derivative terms become singular at the critical latitude, but it can be seen here that this singularity is not realized in finite time because the group velocity (and hence the westward energy flux) of the emitted Rossby waves goes smoothly (rather than discontinuously) to zero as the critical latitude is approached. Grimshaw and Allen (1988) provide a very complicated analysis of the frequency-domain solution of the equations at the critical latitude. The (time domain) considerations here suggest that the complexity may be related to the fact that, at the critical latitude, the vanishing of the Rossby wave group velocity suggests that the periodic solution will require an infinite amount of time to set up.

The results of a one-dimensional, time-dependent, dispersive QG model are presented as the last curve in Fig. 1. The amplitude of the transfer function was taken as the average of the absolute values of the solution extrema in the interval from -4000 to -1000 km after 16 years of integration. These results resemble the curve based on group velocity most closely and will be discussed in the following section.

5. The 1D, β-plane, QG model

A one-dimensional, time-dependent, fully dispersive QG model was run to examine how the dispersive effects influence the time-dependent solution. It might be expected that the approach to criticality may not be simple, since the group velocity of the Rossby waves vanishes at the critical latitude, and information from the initial turn-on transients of the simulation may never be able to leave the domain of interest.

Three representative solutions of the 1D QG model after 3.45 years of integration are presented in Fig. 2, for forcing periods of two years, one year, and one-half year. For the parameters chosen, the forcing period at criticality is 0.66 years, so the first case is essentially a low-frequency case, the second is transitional, and the third is trapped. In each case, the 1D QG results are compared with the solution of a 2D SWE model (described in the appendix) along the central latitude of the SWE β-plane.

These figures show very good agreement in amplitude and phase between the two models at two-year and one-year periods. The small amplitude differences between the SWE and QG results are due to the increase in the coastal Kelvin wave amplitude during the 1000-km propagation from the southern boundary of the 2D SWE model and the midlatitude of the basin (where the 1D QG model was set up). This Kelvin wave growth will be discussed in section 6. The rather poor phase correspondence for the half-year period forcing is primarily due to the neglect of the y wavenumbers in the dispersion relation, rather than due to time lag between the forcing at $y = -1000$ km and the QG solution at $y = 0$ km. A meridional transect through the solution reveals a y scale of about 130 km, which should decrease the phase speed by approximately $(R_d/L_y)^2 = (30/130)^2 = 5\%$. Plotting the solution of the 1D QG model at a time that is 5% before the SWE solution produces the results shown in the lower right panel of Fig. 2, which are in excellent agreement with the SWE model in the interior.

It is clear, then, that the 1D QG model, tuned to the local value of the deformation radius at its latitude and forced by the QG approximation to the coastal Kelvin wave, is capable of very good approximations of the solutions to the SWEs at sufficiently low frequencies. It is now time to turn our attention to the question of the y dependence of the coastal Kelvin wave that forces this system, and its influence on the y dependence of the interior Rossby wave solution.

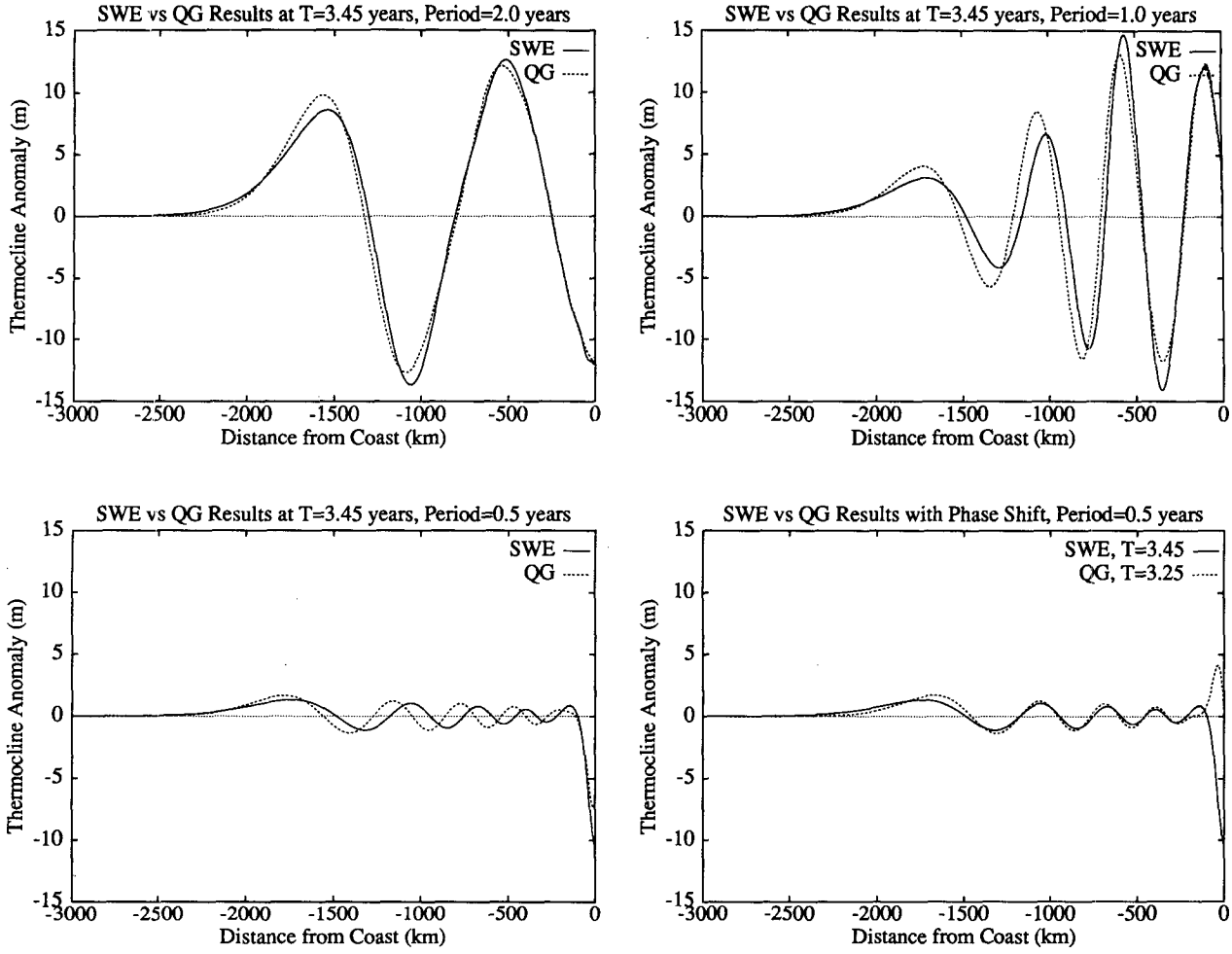

FIG. 2. Solution of the 1D QG model and the SWE model at the central latitude of a β-plane ocean after 3.45 years of forcing with various coastal Kelvin wave forcing periods. The Kelvin wave amplitude is 12 m. See text for discussion.

6. Energy flux analysis

The treatment of the Kelvin wave as a forcing term (rather than as part of a unified solution) helps clarify the Rossby wave generation mechanism in terms of QG dynamics, but removes the feedback by which the Kelvin wave's amplitude is controlled. (See Grimshaw and Allen 1988 for a comprehensive analysis of the unified system at low frequencies.) This feedback can be recovered (at least approximately) by considerations of conservation of energy flux. The energy flux density of a coastal Kelvin wave is (Gill 1982)

$$F_K = \frac{\rho_0 g^2 H}{4 f_0} \eta_K^2, \tag{17}$$

while the energy flux of the interior Rossby waves is (neglecting the y wavenumber l)

$$F_R = \frac{g\rho_0 \eta_R^2}{4} [1 + (kR_d)^2] \left[\frac{-\beta(-k^2 + \gamma^2)}{(k^2 + \gamma^2)^2} \right]. \tag{18}$$

The terms in the first brackets are the PE and KE energy densities, while the second bracket contains the x-directed group velocity. For the midlatitude parameters chosen here, the *maximum* value of F_R/F_K is about 3×10^{-7}, clearly indicating that the leakage is weak. This may be quantified by examining the ratio of the Kelvin wave energy density

$$E_K = \tfrac{1}{4} \rho_0 g R_d \eta_K^2 \tag{19}$$

to the Rossby wave energy flux. An ordinary differential equation for the y dependence of η_K^2 may be set up directly. Making use of $d/dt = cd/dy$, one obtains

$$\frac{d}{dy}(\eta_K^2) = \frac{\beta}{f_0 + \beta y} \eta_K^2 - \frac{f_0 + \beta y}{c^2} [1 + (kR_d)^2] \left[\frac{\beta(-k^2 + \gamma^2)}{(k^2 + \gamma^2)^2} \right] \eta_R^2. \tag{20}$$

The first term on the rhs is the positive change in η_K^2

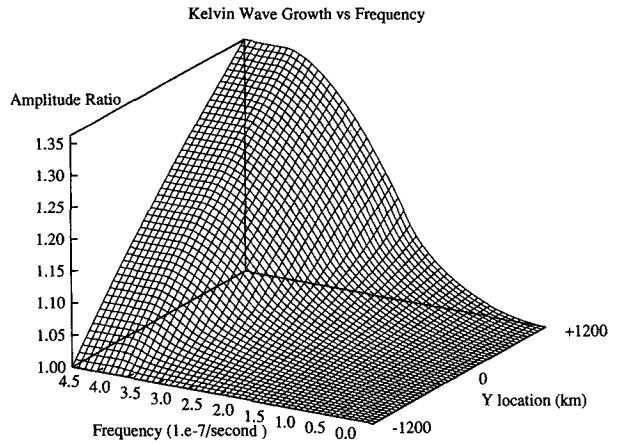

FIG. 3. Increase in the squared amplitude of the coastal Kelvin wave as a function of frequency and y, based on energy flux conservation. The function is independent of frequency above the critical frequency of 4×10^{-7} s^{-1} and asymptotes to no growth for low frequencies.

due to the decrease in R_d, while the second term is the negative change due to energy loss into the Rossby wave field. In the low-frequency regime, we may use the long-wave approximation (7) to obtain the simplified equation

$$\frac{d}{dy}(\eta_K^2) = \frac{\beta}{f}(\eta_K^2 - \eta_R^2) \approx 0 . \qquad (21)$$

We have already noted that $\eta_K = \eta_R$ in the low-frequency limit, so these terms approximately cancel in the domain where the low-frequency/long-wave model is valid. At higher frequencies, the Rossby wave energy flux decreases, leading to an increase in η_K^2 with y. For frequencies above the critical frequency, the energy is completely coastally trapped, and the solution to (20) is linear in y. Thus, η_K is proportional to $\sqrt{f_0 + \beta y}$, as previously shown by Moore (1968) and many others.

For frequencies between the low-frequency regime and the trapped regime, the y dependence of η_K is more complicated, but it varies smoothly between the two extremes. The relation between η_R and η_K is assumed to be the same as that obtained by the analytical solution of the long-wave model, (8), with the phase speed replaced by the Rossby wave group velocity for each frequency. The closed-form solution of (20) is awkward to work with, since the term corresponding to the Rossby wave energy flux must be removed from the equation poleward of the critical latitude for each frequency. The equation must therefore be solved in two domains, one subcritical and one supercritical, with a dividing line that is a function of y and ω, and at which the solutions must be patched together. Rather than deal with this messy (and unenlightening) form of the solution, an adaptive fifth-order Runge–Kutta scheme was used to integrate (20) for a region of ω–y space. The results are presented in Fig. 3. The three regimes are visible here: 1) a high-frequency regime (above 4×10^{-7} s^{-1}) for which the growth is nearly linear in y and independent of frequency, 2) a transitional regime, and 3) a low-frequency regime of (asymptotically) no growth (below about 0.5×10^{-7} s^{-1}).

The predictions of this analysis are in nearly perfect agreement with the results of the SWE model. The ratio of the amplitudes of the incoming and outgoing Kelvin waves are presented in Table 1 along with the theoretical estimates from the numerical integration of (20).

In reference to a claim made earlier, we note that at low frequencies, this result shows that the characteristic scale for the Kelvin wave's variation in y is no smaller than the β scale f_0/β, which is of the order of the planetary radius, so that y wavenumbers are always negligible compared to γ—at least away from the critical latitude and near the eastern boundary. In the interior, the y scale decreases due to β dispersion, but this does not effect the scattering process, per se. In addition, the SWE experiments discussed below show that the decreasing y scale contributes only modest perturbations to the westward phase velocity of the interior field.

7. Discussion

It is perhaps not widely understood that the commonly used midlatitude QG equations contain an approximation to the Kelvin wave solution of the SWEs. The approximation arises from the "consistency condition" derived by McWilliams (1977) and explored by Flierl (1977) and Pinardi and Milliff (1989). The consistency condition may be derived most easily by noting that the QG vorticity equation is subject to a lateral boundary condition that specifies that the streamfunction is constant along the boundary (leading to no normal flow) but that this constant is an unknown function of time. The standard method of solution is to split the equation into two equations: one with a forced interior, but homogeneous boundary conditions; and the other with an unforced interior, but a temporally varying, spatially constant boundary condition. The solution of this latter equation is the QG equivalent of the coastal Kelvin wave. It is characterized by exponential decay away from the bound-

TABLE 1. Predicted and observed growth in the coastal Kelvin wave amplitude during the 2400-km transit along the model's eastern boundary.

Period (years)	SWE ratio	Theory ratio
2.0	1.016	1.017
1.0	1.077	1.080
0.5	1.356	1.350

aries, and arbitrary frequency. This can be seen by examining the QG dispersion relation

$$(k^2 + l^2 + \gamma^2)\omega = -\beta k . \qquad (22)$$

In this form, it is clear that a solution ($k = 0$, $l = i\gamma$) reduces to the identity $0 = 0$, independent of ω. The roles of k and l can be interchanged on the f plane, but not on the β plane. The nonzero rhs of the equation for ($k = i\gamma$, $l = 0$) is precisely the mechanism by which the QG approximation to the Kelvin wave is coupled to the interior solution, just as in the vorticity equation (5).

In a closed basin, the unknown amplitude of the boundary-forced solution can be used to enforce global mass conservation, while in a partially open basin, it can be used to allow coastal Kelvin wave forcing. The inclusion of the QG approximation to Kelvin waves in open boundary models has been suggested briefly by Pinardi and Milliff (1989) and Milliff (1990), but the technique does not appear to have been used in any actual modeling applications.

The locally 1D QG model employed in the comparisons here differs in one crucial way from the traditional QG model, in that it allows the radius of deformation (in the vortex stretching term) to vary with latitude. The neglect of this variation in traditional QG models has been based on its scaling as $O(\beta y/f_0)$. This is reasonable for the investigation of mesoscale features, but can generate O(1) errors for the basin-scale response. The magnitude of this error may be seen in Fig. 4, which contrasts the maximum Rossby wave phase speed for spherical coordinates, the SWE β plane, and the QG β plane. Even in a relatively small model domain of 20° latitude range, the correct Rossby wave maximum phase speed varies by a factor of approximately 4, while the QG β plane assumes a constant value.

The contrasting behavior of the traditional QG, generalized QG [using (5)], locally 1D, QG, and SWE models may be seen in Fig. 5. All four cases used one-year forcing periods, which is an intermediate frequency for this range of latitudes—dispersion is important, but the critical latitude is outside the domain. The SWE model was forced via the coastal waveguide in the SE corner, while the QG models were forced uniformly all along the eastern boundary. Aside from some artifacts near the northern and southern boundaries (where the models were specified with slightly different boundary conditions), the SWE, generalized QG, and 1D QG results are remarkably similar. The largest differences in the interior appear to be some small phase errors in which the generalized QG and 1D QG models lead the SWE solution slightly. The slight differences are likely due to the neglect of the smaller forcing terms in the vorticity equation, rather than due to the QG approximation itself. (Although it is not shown here, the inclusion or neglect of the $2\beta/f\eta_{yt}$ term in the vorticity equation makes no visible

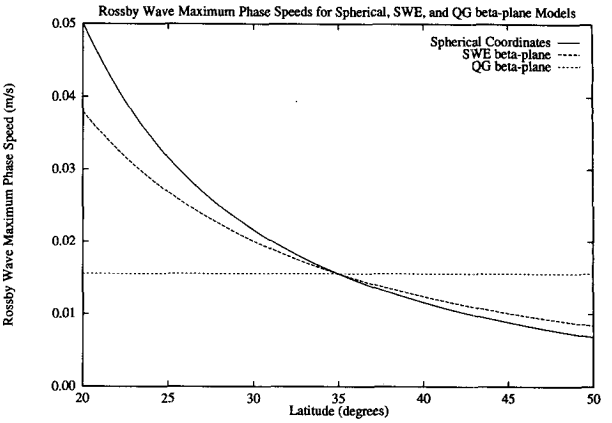

FIG. 4. Maximum Rossby wave phase speeds for spherical coordinates, for the SWE β-plane, and for the traditional QG β-plane.

difference in the solution for these parameters.) In contrast, the traditional QG model produces qualitatively different results, as expected from Fig. 4. It is expected that balance equation models (which retain the full variation of the Coriolis parameter) will perform well here and may be more accurate than the generalized QG model. At least some balance equation models contain a low-frequency approximation to the Kelvin wave, and so they simply need to be forced correctly at the input to the coastal waveguide (Gent and McWilliams, 1983a,b).

The importance of the meridional variation in long-wave phase speed of these Rossby waves relative to the general circulation and energetics of the region is not entirely clear. On the one hand, even though the variations are O(1) relative to the O(2) cm s^{-1} middomain long-wave phase speed, they are likely to be small relative to the Doppler shifts created by advection due to the O(10) cm s^{-1} mean Sverdrup circulation. An analysis of the interaction between long wind-generated Rossby waves and the Sverdrup flow is presented in Dewar (1989) and could easily be generalized to include forcing from coastal Kelvin waves. On the other hand, recent satellite observations and numerical model results have shown clearly that the Rossby wave emitted by the 1982–83 El Niño remained coherent for a full decade at midlatitudes while propagating across the entire width of the North Pacific Ocean (Jacobs et al. 1994). It is clear from the pattern of the Rossby wave observed in 1993 that the meridional variation in phase speed is an O(1) part of the dynamics. The Rossby wave was less clearly defined and coherent in the South Pacific Ocean for the same period.

For regions not influenced by large, low-frequency coastal Kelvin waves, the entire process is possibly of negligible importance. In a closed computational domain, however, the Kelvin waves may carry significant energy around the basin. Cox (1987) speculates that a significant source of low-frequency variability in his

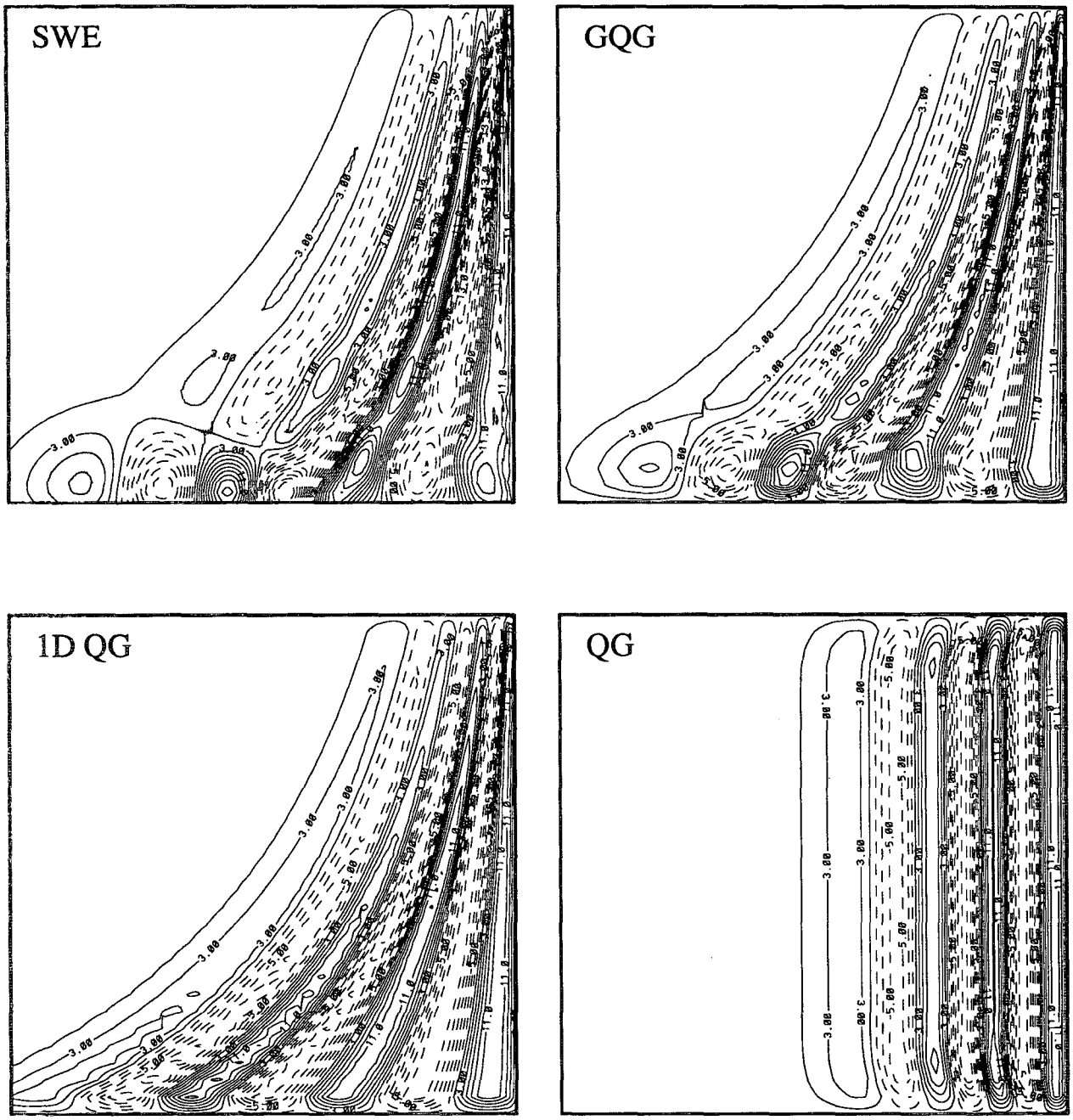

FIG. 5. Thermocline anomaly fields after 3.45 years for the SWE model, the generalized QG model, the composite of the locally 1D QG models, and the standard QG model. The forcing period was 1 year. All figures use the same scaling and contour intervals with a domain size of 4000 km E–W by 3000 km N–S.

numerical simulation of a closed basin may be dependent on the Kelvin wave scattering process. He hypothesizes that the emitted Rossby waves interact with the interior solution to produce pressure signals on the western boundary. These are then rapidly propagated back to the eastern boundary, where they emit more Rossby waves to repeat the process. Unfortunately, the results were not adequate to distinguish between Kelvin wave propagation and advection as "fast" mechanisms to move the energy back eastward. In a more direct study of these dynamics, the boundary pressure adjustment (and subsequent Kelvin wave scattering process) due to the interaction of a monopole vortex with the western boundary in a closed domain is examined by Milliff and McWilliams (1994) using both QG and SWE models. Although the meridional variations in

phase speed demonstrated in Fig. 5 are clear in their SWE results and absent in their QG results, it is not clear that the amplitude of the Kelvin waves and the emitted Rossby waves are large enough to significantly modify a wind-driven interior solution.

8. Summary

The results presented here have shown that the inclusion of a simple approximation to the forcing of Rossby waves by coastal Kelvin waves is capable of representing some aspects of the low-frequency Kelvin wave scattering process. In particular, in the low-frequency regime, the amplitudes of both the Kelvin wave and the emitted Rossby wave are both approximately correct for domains of modest meridional scale. As the frequency shifts into the transitional regime, the coastal Kelvin wave grows in amplitude as it propagates poleward, and the assumption of y-independent coastal sea level in the QG model becomes increasingly inaccurate. More importantly, the QG assumption of constant deformation radius, and hence constant maximum Rossby wave phase speed, results in O(1) errors in the westward phase velocity and energy flux of the emitted Rossby waves.

The inclusion of the variation of the deformation radius in the vortex stretching term provides a y-dependent long-wave phase speed and allows the model to fairly accurately reproduce the behavior of the β-plane SWEs. None of the other terms that are formally of the same order have a similarly large impact on the quality of the solution. Because of the strong, low-frequency coastal Kelvin wave signal in the eastern Pacific Ocean, it is recommended that simulations of that region employ dynamical approximations that properly include this meridional variation in the baroclinic long-wave phase speed.

Acknowledgments. This work began in 1989 while the author was at the Florida State University, completing his Ph.D. under the direction of Secretary of the Navy Professor James J. O'Brien, and supported by a PACER Fellowship from Control Data Corporation. The work was completed at the University of Delaware under the support of the National Science Foundation Contract OCE-9206176. I would like to thank Dr. Gerald Browning for help with the specification of the open boundary conditions, and Dr. Ralph Milliff and Dr. James C. McWilliams for several helpful discussions.

APPENDIX

The Shallow-Water Equation Model

A linear, reduced-gravity shallow-water model was configured as a midlatitude β-plane model with closed boundaries on the east and west. (The model was closed on the western boundary because of technical difficulties with specifying two adjacent open boundaries.) The model was forced by a Kelvin wave on the incoming characteristic at the southern boundary. The information on the outgoing characteristic was calculated from the interior solution at both open boundaries. At the northern boundary the wave on the incoming characteristic was specified to have zero amplitude. The domain size was 4000 km E–W by 3000 km N–S, with 10-km resolution in x and 60-km resolution in y. Buffer zones of constant Coriolis parameter were maintained for the 300-km (five-grid intervals) bands adjacent to the northern and southern boundaries in order to ensure the stability of the open boundary conditions. Between the buffer zones, the Coriolis parameter was varied linearly about a mean value $f_0 = 8 \times 10^{-5}$ s^{-1}, with a slope of $\beta = 2 \times 10^{-11}$ m^{-1} s^{-1}. The reduced gravity and upper-layer depth were chosen to provide a $c = 2.4$ m s^{-1} gravity wave phase speed. The associated internal radius of deformation $R_d \equiv c/f$ varied from 43 km at the southern boundary to 23 km at the northern boundary.

REFERENCES

Anderson, D., and Gill, A., 1975: Spin-up of a stratified ocean, with applications to upwelling. *Deep-Sea Res.*, **22,** 583–596.

——, and Rowlands, P., 1976: The role of inertia–gravity and planetary waves in the response of a tropical ocean to the incidence of an equatorial Kelvin wave on a meridional boundary. *J. Mar. Res.*, **34**(3), 295–312.

Auad, G., Pares-Sierra, A., and Vallis, G. K., 1991: Circulation and energetics of a model of the California Current system. *J. Phys. Oceanogr.*, **21,** 1534–1552.

Clarke, A. J., 1992: Low-frequency reflection from a nonmeridional eastern ocean boundary and the use of coastal sea level to monitor eastern Pacific equatorial Kelvin waves. *J. Phys. Oceanogr.*, **22,** 163–183.

——, and C. Shi, 1991: Critical frequencies at ocean boundaries. *J. Geophys. Res.*, **96,** 10 731–10 738.

Cox, M. D., 1987: An eddy-resolving model of the ventilated thermocline: Time dependence. *J. Phys. Oceanogr.*, **17,** 1044–1056.

Cummins, P., and L. Mysak, 1988: A quasi-geostrophic circulation model of the northeast Pacific. Part I: A preliminary numerical experiment. *J. Phys. Oceanogr.*, **18,** 1261–1286.

Dewar, W. K., 1989: A nonlinear, time-dependent thermocline theory. *J. Mar. Res.*, **47,** 1–31.

Enfield, D., and J. Allen, 1980: On the structure and dynamics of monthly mean sea level anomalies along the Pacific Coast of North and South America. *J. Phys. Oceanogr.*, **10,** 557–578.

Flierl, G. R., 1977: Simple applications of McWilliams' 'A note on a consistent quasigeostrophic model in a multiply connected domain.' *Dyn. Atmos. Oceans,* **1,** 443–453.

Gent, P., and J. McWilliams, 1983a: The equatorial waves of balanced models. *J. Phys. Oceanogr.*, **13,** 1179–1192.

——, and ——, 1983b: Consistent balanced models in bounded and periodic domains. *Dyn. Atmos. Oceans,* **7,** 67–93.

Gill, A. E., 1982: *Atmosphere–Ocean Dynamics,* Vol. 30. *Int. Geophys. Ser.,* Academic Press, 662 pp.

Grimshaw, R., and J. Allen, 1988: Low-frequency baroclinic waves off coastal boundaries. *J. Phys. Oceanogr.*, **18,** 1124–1143.

Jacobs, G. A., H. E. Hurlburt, J. C. Kindle, E. J. Metzger, J. L. Mitchell, W. J. Teague, and A. J. Wallcraft, 1994: Decade-scale trans-Pacific propagation and warming effects of an el niño anomaly. *Nature,* **370**(6488), 360–370.

Johnson, M. A., and J. J. O'Brien, 1990: The northeast Pacific Ocean response to the 1982–1983 El Niño. *J. Geophys. Res.*, **95**(C5), 7155–7166.

McCreary, J., 1976: Eastern tropical ocean response to changing wind systems: With application to El Niño. *J. Phys. Oceanogr.*, **6,** 632–645.

McWilliams, J. C., 1977: A note on a consistent quasigeostrophic model in a multiply-connected domain. *Dyn. Atmos. Oceans,* **1,** 427–441.

Meyers, G., 1979: On the annual Rossby wave in the tropical North Pacific Ocean. *J. Phys. Oceanogr.*, **9,** 663–674.

Milliff, R., 1990: A modified capacitance matrix method to implement coastal boundaries in the Harvard Open Ocean Model. *Math. Comput. Simul.*, **31**(6), 541–564.

——, and J. C. McWilliams, 1994: The evolution of boundary pressure in ocean basins. *J. Phys. Oceanogr.*, **24,** 1317–1338.

Moore, D. W., 1968: Planetary-gravity waves in an equatorial ocean. Ph.D. thesis, Harvard University, 201 pp.

Pares-Sierra, A., and J. O'Brien, 1989: The seasonal and interannual variability of the California Current system: A numerical model. *J. Geophys. Res.*, **94**(C3), 3159–3180.

Pinardi, N., and R. F. Milliff, 1989: A note on consistent quasigeostrophic boundary conditions in partially open, simply and multiply connected domains. *Dyn. Atmos. Oceans,* **14,** 65–76.

Roden, G., 1977: On long-wave disturbances of dynamic height in the North Pacific. *J. Phys. Oceanogr.*, **7,** 41–49.

Shriver, J. F., M. A. Johnson, and J. J. O'Brien, 1991: Analysis of remotely forced oceanic Rossby waves off California. *J. Geophys. Res.*, **96**(C1), 749–757.

White, W., 1977: Annual forcing of baroclinic long waves in the tropical North Pacific Ocean. *J. Phys. Oceanogr.*, **7,** 50–61.

——, and J. Saur, 1981: A source of annual baroclinic waves in the eastern subtropical North Pacific. *J. Phys. Oceanogr.*, **11,** 1452–1462.

——, and ——, 1983: Sources of interannual baroclinic waves in the eastern subtropical North Pacific. *J. Phys. Oceanogr.*, **13,** 531–544.

Williams, G. P., 1985: Geostrophic regimes on a sphere and a beta plane. *J. Atmos. Sci.*, **42,** 1237–1243.